AN50004

Using power MOSFETs in DC motor control applications

Rev. 1.1 — 2 March 2021 application note

Document information

Information	Content
Keywords	DC motor, MOSFET
Abstract	This application note aims to give some general insights into how to drive a DC motor using Nexperia Power MOSFET devices

nexperia

1. Introduction

Within the automotive environment, brushed Direct Current (DC) motors play an important role in the control of many applications within the car such as mirror folding control, window lifter, seat control, sunroof and power tailgate control, as well as oil, fuel and water pumps. Some may be identified in Fig. 1 below.

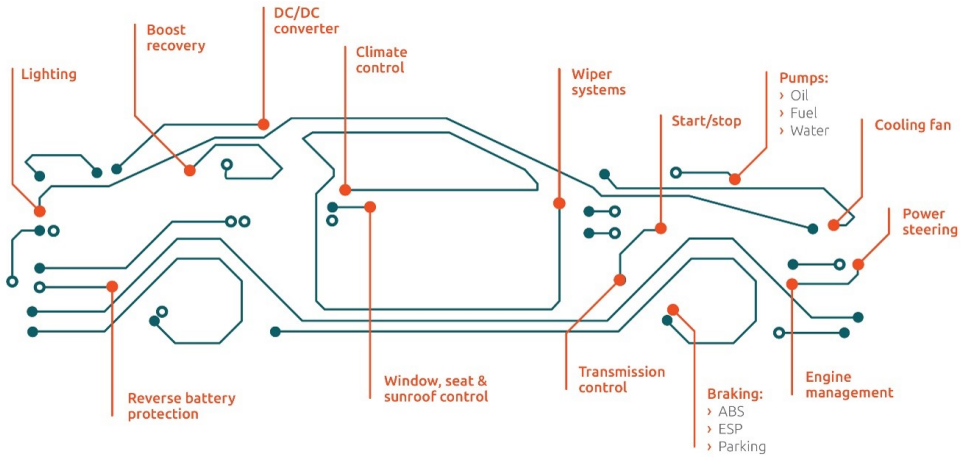

Fig. 1. Automotive applications

In this application note some Nexperia automotive H-bridge applications will be exemplified. Moreover, the theory behind the H-bridge circuit will be discussed and some circuit examples will be given. Lastly, MOSFET recommendations will be given for some of the applications found in a car.

2. Applications

As mentioned there are several applications in the automotive field which use DC brushed motors. Within this chapter an example of a relay replacement demo will be given within a power-folding mirror assembly. Additionally, other automotive applications which use MOSFETs in half-bridge and H-bridge configurations for motor control, will be given.

2.1. Relay replacement in a power-folding mirror assembly

In modern automotive applications, an average of about 30 relays are used in a car. Driving a relay is simple, and the internal resistance of the connection can be very low. However, compared with relays, MOSFETs have obvious advantages in noise, service life, miniaturization and reliability. Therefore more and more manufacturers consider using MOSFETs to replace relays.

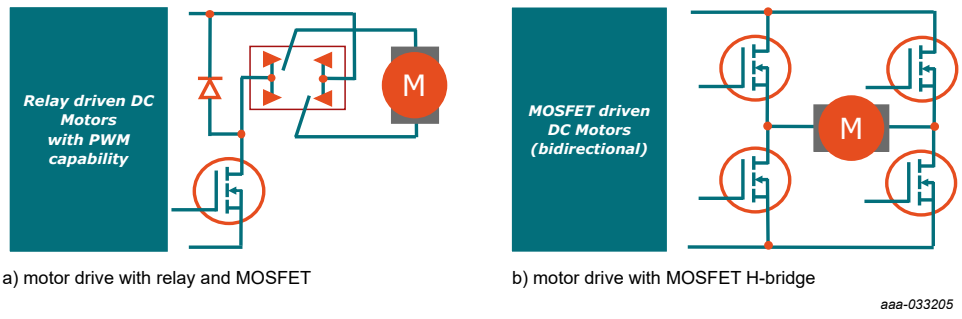

Fig. 2. Relays replaced with MOSFETs

Fig. 2 a) is a motor scheme that mainly uses relays for motor drive. The direction of the motor rotation is selected by the contact of the relay. However, the relay cannot control the current of the

motor, so it might still need to be connected to a MOSFET to have a more reactive and precise control against current changes, so as, for example, to meet functional requirements of anti-pinch.

Fig. 2 b) is a scheme that directly uses MOSFETs to drive the motor. The direction of motor rotation can be controlled using only one MOSFET, while the other MOSFET can be switched by PWM to control the motor current. A demo board may be seen in Fig.3.

A Nexperia demo application which showcases how MOSFETs can replace relays may be seen in Fig. 4. These were used in controlling the mirror power-folding mechanism using 12 V or 24 V H-bridge DC motor control. As can be seen, the relays were replaced with MOSFETs in the LFPAK33, LFPAK56D and LFPAK56 small SMD packages.

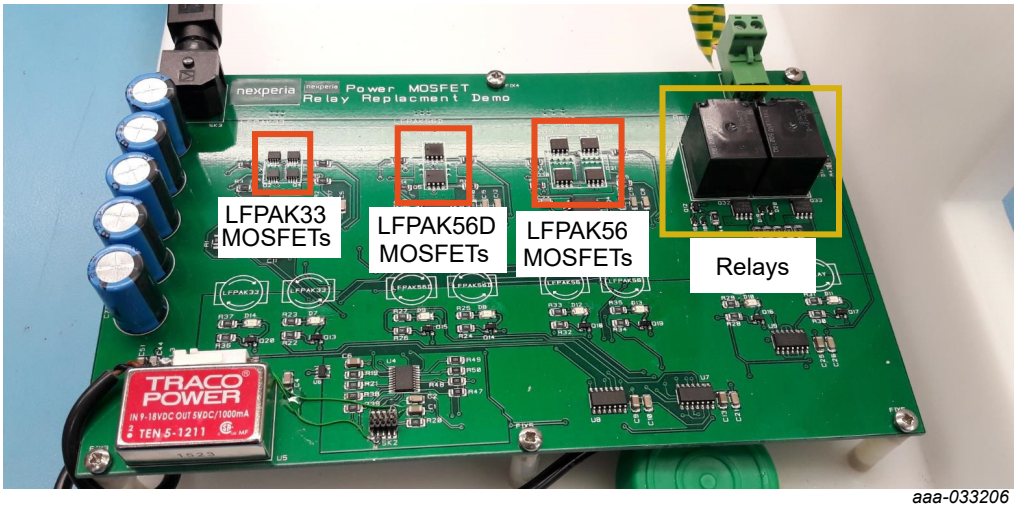

Fig. 3. Relay replacement demo board

Fig. 4. Demo board driving a mirror folding mechanism

By using any of the power MOSFET variants, there will be a space reduction of up to 1:100 in terms of volume, 1:10 in terms of board area and 1:20 in terms of weight. This is depicted by the orange highlighted area in Fig. 3 versus the yellow highlighted area. In terms of performance, the LFPAK MOSFETs will offer high current handling for locked rotor protection, high reliability and full Automotive Qualification AEC-Q101. Lastly, the copper clip within the LFPAK MOSFETs offers a good thermal performance.

2.2. Other applications

As seen in Fig. 1, window lifter, seat control, sunroof and power tailgate control as well as oil, fuel and water pumps are other automotive applications using power MOSFETs in H-bridge configurations. Due to this an overview of a H-bridge motor controller and its theory is given in the next chapters as well as results of a simulation emulating the behaviour of the application seen in the Nexperia technical note *TN90002*.

3. Theory and circuit simulation

3.1. Brushed Direct Current motor modelling

The DC motor is a common actuator in the automotive environment and in order to understand how to better choose the MOSFETs controlling it and their ratings as well as obtain the wanted behaviour from the motor, it was modelled below. Moreover, as it will be seen in further chapters the motor characterisation was conducted in order to have a representative example.

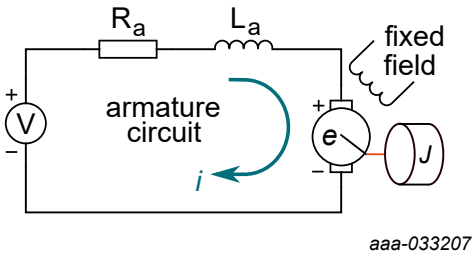

Fig. 5. Motor armature equivalent circuit

In Fig. 5 the electric circuit of the DC motor armature is depicted. It shows its electric resistance (R_a), inductance (L_a) as well as back EMF (e). Moreover, the rotor mechanical constants are also shown as: motor torque (T), rotor angle (θ) and rotor inertia (J). Taking these into consideration and applying some circuit analysis techniques such as Kirchhoff's voltage law, gives Eq. 1 below:

$$V = i \times R_a + L_a \frac{di}{dt} + e \tag{1}$$

In this case *V* is the input voltage to the DC motor and the one supplied by the H-bridge which is formed by 4 MOSFETs within 2 half-bridges in order to obtain bi-directional control. More details are given in Section 3.2.

Considering the magnetic field as constant the torque produced by the DC motor will thus be proportional to the armature current and the motor torque constant K_T. This may be seen in Eq. 2:

$$T = K_T \times i \tag{2}$$

Moreover, the back EMF is proportional to the rotor velocity $\dot{\theta}$ and the back EMF constant K_e, as shown in Eq. 3 below:

$$e = K_e \times \frac{d\theta}{dt} = K \times \omega \tag{3}$$

As it is considered that the torque and back EMF constants are equal, the following equality may be given: $K_T = K_e = K$.

Lastly Eq. 4 and Eq. 5 relate the electrical and mechanical domains which describe the behaviour of the motor:

$$\text{Mechanical domain: } J\frac{d^2\theta}{dt^2} = T - D\frac{d\theta}{dt} \Rightarrow \frac{d^2\theta}{dt^2} = \frac{1}{J}\left(K_T \times i - D\frac{d\theta}{dt}\right) \tag{4}$$

$$\text{Electrical domain: } L_a\frac{di}{dt} = V - iR_a - e \Rightarrow \frac{di}{dt} = \frac{1}{L_a}\left(V \times iR_a - K_e \times \frac{d\theta}{dt}\right) \tag{5}$$

Based on the above equations the motor output torque and speed may be approximated by knowing the motor constants. This may be found using the motor data sheet or by measurement. More information about how some of the constants were determined for an example DC motor may be found in Section 5.

3.2. H-bridge theory

The H-bridge, also known as full-bridge, is an electronic system consisting of four switches and capable of creating a bi-directional current and reversible voltage across its load. This function comes in handy when driving a motor because it allows a change in the direction of its rotation and, if the application allows it, even to use it as a generator. This circuit is used in many systems such as in inverters (DC/AC), regulators (DC/DC) and class-D amplifiers.

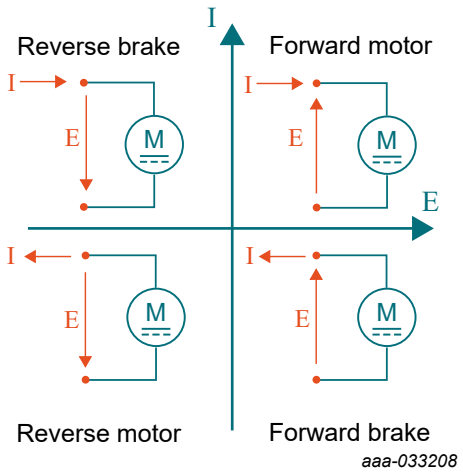

Fig. 6. Motor direction and braking control

The H-bridge can be thought of as composed of two half-bridges used simultaneously. The H-bridge allows the motor to work as a generator in both directions of rotation therefore it is considered a 4-quadrant converter. The half-bridge is capable of bi-directional current but not reversible voltage and thus is considered a 2-quadrant one. Therefore, the latter is mainly used in motor drive applications with single-direction motors such as oil pump motors and small fans. Another difference between the two types of circuits is the voltage output for a given supply voltage, that is the amplitude of the voltage applied to the load. It is double that of the DC link in case of a H-bridge, and exactly V_{DC} in case of the half-bridge.

3.3. Modes of switching

The easiest and most popular way to drive a DC motor using a H-bridge is by using pulse width modulation (PWM). Here the MOSFETs are switched at a constant frequency with a control signal having variable duty cycle. This allows the average voltage across the motor to vary and thus control the rotor angular velocity. The MOSFETs in a H-bridge can be switched in different sequences to provide the desired voltage polarity. There are two common modes: bipolar and unipolar.

3.3.1. Bipolar drive

The bipolar drive allows two MOSFETs to be switched ON at a time, see Fig. 7. For example for positive current (from node A to node B) both Q2 and Q3 are turned ON. Whereas, for negative current, Q1 and Q4 are turned ON. By switching these two pairs the direction of the current can be controlled thus applying a voltage across the motor that varies between V_{DC} and $-V_{DC}$, with an average value that depends on the duty cycle (δ). Timing is very important in this mode. A time delay, known as dead-time, must be set between the turning OFF of one pair and the turning ON of the other pair, in order to avoid cross-conduction (or shoot through), that is shorting the supply, as shown in Fig. 8. This time delay can go from several nanoseconds to around 5 µs and, in this

latter case, it will limit the switching frequency to approximately 20 kHz. Even though safer, a longer dead-time may cause non-linear output with respect to the PWM and lower efficiency. Reducing the dead-time is a matter of knowing and predicting the input parameters of the MOSFETs in use. In particular a longer dead-time will be required for a device with larger gate charge because of the longer intrinsic fall time. Besides temperature variations and parameter spread should be taken into account if a very small dead-time is needed [1].

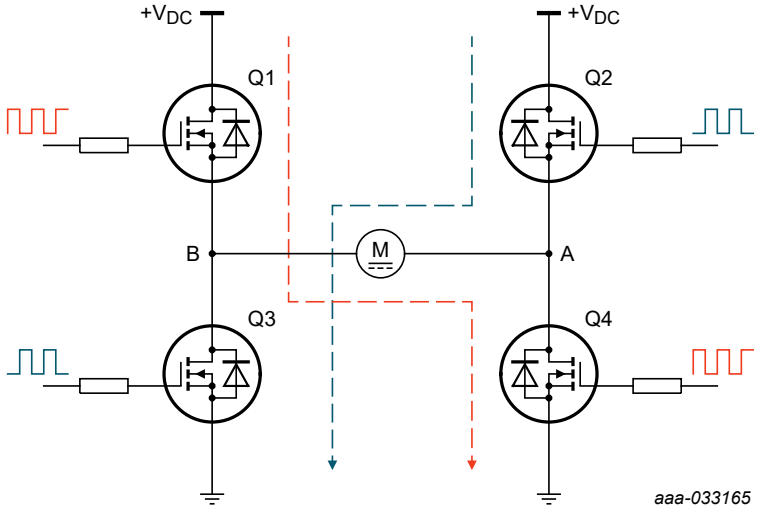

Fig. 7. Bipolar drive H-bridge switching

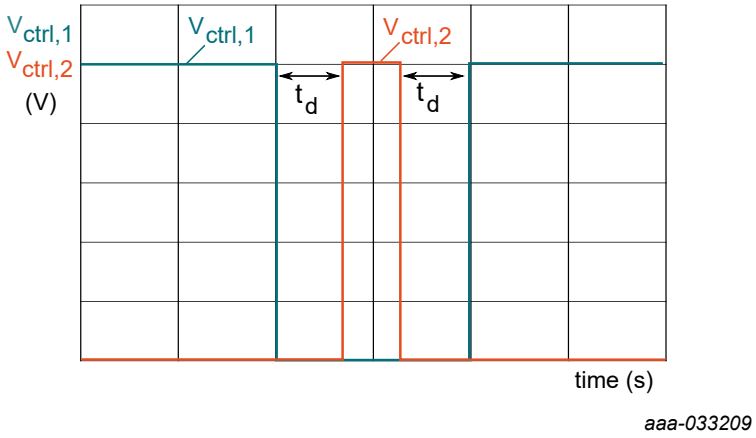

Fig. 8. Bipolar drive H-bridge switching dead-time

Due to the magnetic field build up in the motor, during the delay phase some current will continue to flow, even though all the devices are turned OFF, by recirculating through the MOSFETs body diodes. If we assume a negative current through the motor, then during the delay phase it will flow through Q2 and Q3 body diodes.

Table 1 shows the switching sequence and the outcome of this drive scheme:

Table 1. MOSFET switching sequence

Phase	MOSFETs ON	MOSFETs OFF	V_{in}
A	Q2, Q3	Q1, Q4	V_{DC}
Delay	-	Q1, Q2, Q3, Q4	$-V_{DC} + 2\ V_D$ for $I_m > 0$ $V_{DC} - 2V_D$ for $I_m < 0$
B	Q1, Q4	Q2, Q3	$-V_{DC}$

Simply by looking at the waveforms of motor voltage and current Fig. 9 it is possible to find out how the motor current ripple (Δi_L) varies with respect to motor and driver parameters. For this analysis

we will assume, for simplicity, a steady state condition with the motor spinning at a constant velocity.

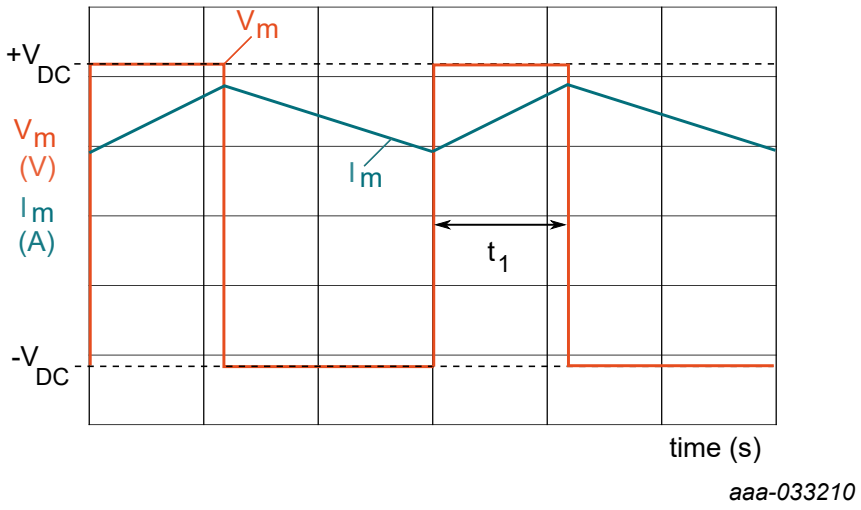

Fig. 9. Bipolar drive voltage and current ripple waveforms

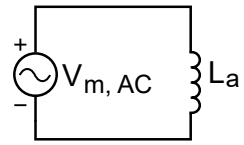

Fig. 10. Armature inductance

Besides we will need to separate the AC from DC component. By doing this we obtain the circuit in Fig. 10 where La is the inductance of the motor. The ripple can then be approximated as:

$$\Delta i_{L_a} = \frac{\Delta v_{L_a}}{L_a} \Delta t \tag{6}$$

Where:

$$\Delta v_{La} = V_{m,AC} = V_{amp} - V_{m,avg} = 2V_{DC} - 2V_{DC}\,\delta = 2V_{DC}(1-\delta) \tag{7}$$

$$\Delta t = t_1 = \frac{\delta}{f_{SW}} \tag{8}$$

Where V_{amp} is the amplitude of the motor voltage, $V_{m,avg}$ its average value and f_{sw} the switching frequency. If we substitute the two parameters in the first equation we obtain:

$$\Delta i_{L_a} = V_{DC} \frac{2(1-\delta)\,\delta}{L_a\, f_{SW}} \tag{9}$$

The maximum ripple can be found when δ = 50%:

$$\Delta i_{L(max)} = \frac{V_{DC}}{2\, L_a\, f_{sw}} \tag{10}$$

3.3.2. Unipolar drive

The unipolar drive scheme, instead, allows for the elimination of the dead time which reduces the complexity of the driver circuit. This scheme allows for the current to be regulated by keeping ON one high side MOSFET (Q2 or Q4) while switching only one low side MOSFET (Q3 or Q1). The H-bridge will allow the motor to spin in a forward or reverse rotation direction, depending on the pair of MOSFETs selected and the polarity of the motor.

Another difference with the bipolar drive scheme is the fact that the voltage across the motor will have an amplitude of V_{DC}. For the same reason described in the bipolar drive some current will be forced to flow through one of the MOSFETs body diode when the switching MOSFET is turned OFF. If we assume Q3 switching and Q2 turned ON, then when the former is switched off then the current will flow through Q1 body diode. In order to decrease the loss caused by the diode voltage drop then Q1 can be switched ON while Q3 is OFF. In this case a proper dead-time constraint must be respected.

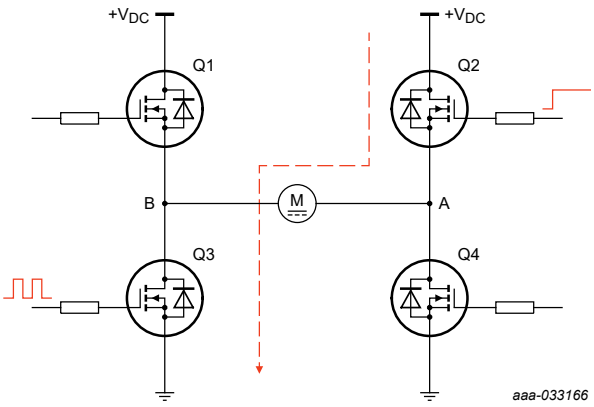

Fig. 11. Unipolar drive H-bridge switching

Table 2 shows the switching sequence and outcome of this drive scheme, in case of forward rotation (positive current).

Table 2. MOSFET unipolar switching sequence

Phase	MOSFETs ON	MOSFETs OFF	V_{in}
A-on	Q2, Q3	Q1, Q4	V_{DC}
B-on	Q2	Q1, Q3, Q4	$-V_D$

In the same way as for the bipolar drive scheme the ripple current can easily be calculated using the same procedure. Starting from Eq 11, this time Δv_{La} will be equal to:

$$\Delta v_{La} = V_{amp} - V_{m,avg} = V_{DC} - V_{DC}(1-\delta) \tag{11}$$

If we substitute Δv_{La} and Δt (which remained unchanged) in Eq. 11 we obtain:

$$\Delta i_{L_a} = V_{DC} \frac{(1-\delta)\,\delta}{L_a\ f_{sw}} \tag{12}$$

The maximum ripple can be found when δ = 50%:

$$\Delta i_{L(max)} = \frac{V_{DC}}{4\ L_a\ f_{sw}} \tag{13}$$

Notice how, this time, the peak of the ripple ends up being half of the one found for the bipolar case.

3.4. MOSFET Dissipation

Power dissipation in a MOSFET employed in a H-bridge is caused by three processes: conduction, commutation and body diode conduction. With the MOSFET fully ON the only source of dissipation is given by its R_{DSon}.

R_{DSon}	drain-source on-state resistance	V_{GS} = 10 V; I_D = 25 A; T_j = 25 °C; Fig. 11		-	2.5	3.5	mΩ
		V_{GS} = 10 V; I_D = 25 A; T_j = 175 °C; Fig. 11; Fig. 12		-	-	6.9	mΩ

Fig. 12. BUK7Y3R5-40E data sheet R_{DSon}

Looking at one single MOSFET the average power over the whole switching period can be expressed as:

$$P_{cond} = I_{D(RMS)}^{2} R_{DSon} \tag{14}$$

Where $I_{D(RMS)}$ is the RMS value of the drain current. The value of on-state resistance varies with the junction temperature (as can be seen in Fig. 12 and Fig. 13), so during design phase a worst case scenario evaluation would be useful in determining the upper limit for this contribution. It's worth noting that the R_{DSon} changes also with respect of V_{GS}, thus over-driving the MOSFET with a higher control voltage will reduce the losses. For example for the BUK7Y3R5-40E it is advised to use $V_{GS} \geq 10$ V, see Fig. 14.

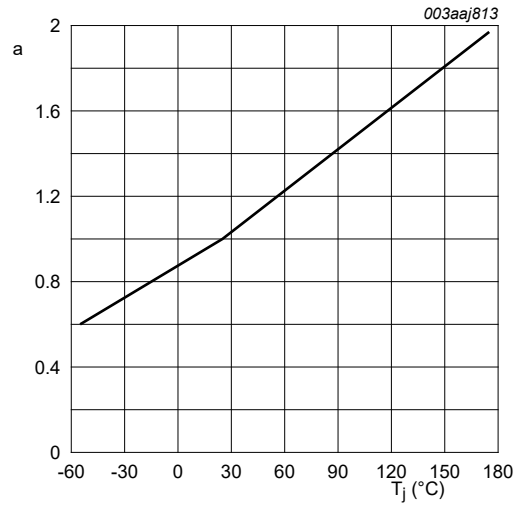

Fig. 13. Normalized drain-source on-state resistance factor as a function of junction temperature

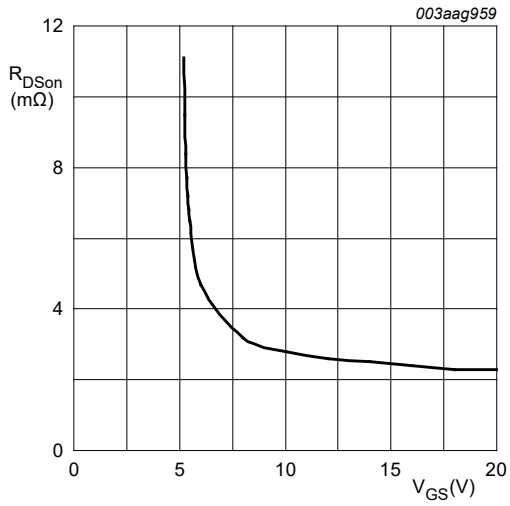

Fig. 14. Drain-source on-state resistance as a function of gate-source voltage; typical values

As with any real device that undergoes commutation, losses are caused by the finite time that the device takes in changing its state, from fully ON to OFF and vice versa. During these transitions the device crosses, even if very briefly, the linear region where it dissipates a significant amount of power. Therefore the total power loss can be written as:

$$P_{sw} = P_{OFF \rightarrow ON} + P_{ON \rightarrow OFF} = \frac{1}{2} V_{DC} I_D t_r f_{sw} + \frac{1}{2} V_{DC} I_D t_f f_{sw} \tag{15}$$

Where t_r and t_f are the rise and fall time, respectively. These will depend on the MOSFET dynamic parameters like threshold voltage V_{th} and gate capacitance.

As previously stated when for example in a unipolar drive scheme the switching MOSFET is turned OFF the current will recirculate through the other switching MOSFET body diode, that is otherwise OFF. In this case the MOSFET will dissipate an average power that depends on the conduction time of the diode and that can be expressed as:

$$P_{BD} = V_D \, I_{S,avg} + I_{S,rms}^2 \, R_D \tag{16}$$

It's worth noting that since we are not dealing with a small signal diode, the power is composed of two components. The first one is given by the forward drop voltage and the average forward current. The other is due to the series resistance of the diode, which can be graphically visualised as the slope of the curve representing I_S versus V_{SD}.

In case of the BUK7Y3R5-40E V_{SD} = 0.4 V (@175 °C) while the series resistance can be calculated considering two points on the curve, obtaining R_D = 2.5 mΩ (see Fig. 15).

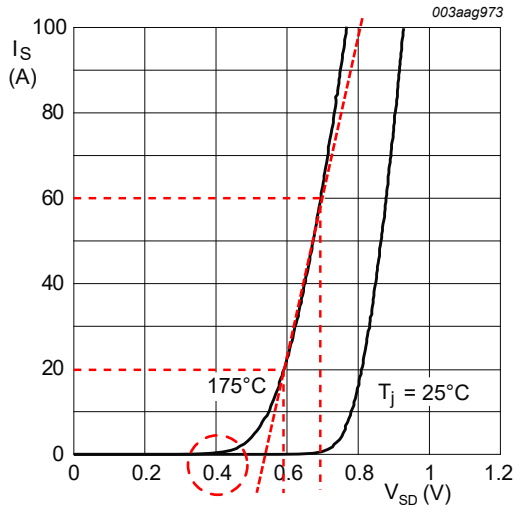

Fig. 15. Source (diode-forward) current as a function of source-drain voltage; typical values

These three types of losses will determine the final junction temperature of the MOSFET, together with the initial ambient temperature, FET and PCB thermal impedances (Z_{th}). A Cauer or Foster model can be used to evaluate it.

The switching frequency, f_{sw}, influences not only the dissipated power of the MOSFETs switching but also that of the motor. Therefore it is important to choose it properly. The frequency must be high enough so that the mechanical actuator is blind to its AC content, passing only DC. On the other hand the upper limit is chosen to minimize losses and non-linearities. The motor effectively acts as a low pass filter having a cut-off frequency equal to:

$$f_c = \frac{1}{2\pi\tau} \tag{17}$$

where τ is the motor time constant. If the switching frequency is above this value then the motor will operate correctly, averaging the PWM signal. As a consequence the time constant of the motor must be known. For better performances the switching frequency should be:

$$f_{sw} \geq 10 f_c \tag{18}$$

The switching period should be also longer than the dead time in order to minimize non-linearities:

$$f_{sw} < \frac{10}{t_d} \quad (19)$$

As previously stated the switching frequency is directly proportional to the commutation losses of the MOSFET, therefore we would choose the frequency to be as low as possible in order to minimize them. On the other hand the frequency has an opposite effect on the current ripple Δi_L, (increases with the frequency), which determines the losses of the motor. Therefore, the final selection must be a compromise between these two conditions [1].

4. H-bridge motor controller design using Nexperia discrete semiconductors and logic ICs

The following design is based on the technical note *TN90002,* and represents an example of how to implement a H-bridge motor controller. This can be particularly useful to identify and understand the main components necessary to drive a DC motor.

The system used here is an example of closed loop electronic drive that employs PWM and selectable switching frequencies to vary the motor shaft speed and it's capable of changing the direction of rotation. It uses a unipolar drive scheme, Fig. 16 and Table 3 summarise the switching scheme and its outcome.

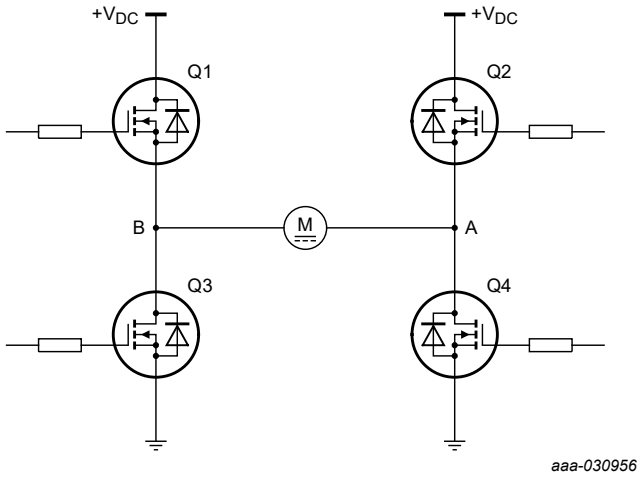

Fig. 16. Simplified H-bridge motor control

Table 3. Switching phases

Motor direction	MOSFET fully on	MOSFET switching	MOSFETs OFF	V_m and I_m
Forward	Q2	Q3	Q1, Q4	($-V_D$, V_{DC}) and $I_m > 0$
Reverse	Q4	Q1	Q2, Q3	($-V_{DC}$, V_D) and $I_m > 0$

The system is composed of the following subsystems:

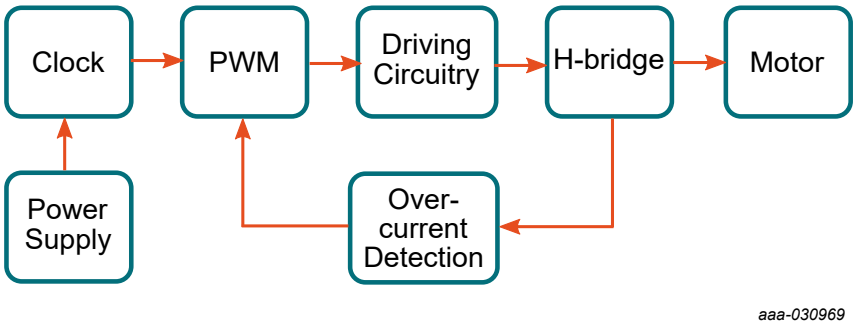

Fig. 17. H-bridge motor controller block diagram

- **Power supply:** in a real application the main source of energy would come from a battery (acid-lead, Li-ion, …). Its voltage is stepped-down using a buck converter in order to create a stable supply for the MOSFETs drivers and accommodates input voltages ranging from 12 V to 48 V. A linear regulator is then used to power the logic devices. Between battery and buck regulator some protection might be included, such as: transient overvoltage and reverse polarity protection (see *AN50001 - Reverse battery protection in automotive applications* for further information).
- **Clock:** timing is needed to control the MOSFETs switching frequency (selectable between 31.3 kHz, 15.6 kHz and 7.8 kHz). Furthermore a crystal oscillator is employed to create a stable and accurate 4 MHz frequency.
- **PWM:** this section consists of PWM enable and reset, dead-time control, level shifting stage and direction selection. The dead time (approximately 2.5 µs) is set using an RC filter and it's applied to the switching MOSFETs (Q1 and Q3) in order to avoid cross-conduction. The duty cycle varies in 8 steps between 0% to 100%.
- **Drivers:** low and high side MOSFETs drivers are used to provide the right amount of V_{GS} and I_G to properly turn ON and OFF the MOSFETs. If an NMOS is used for the high side a suitable circuit is needed in order to create a voltage higher than the supply (so that $V_{GS} > 0$). In this case the choice has fallen on a charge pump. A simple bootstrap function wouldn't be suitable due to the fact that for a duty cycle of 100% there wouldn't be time to recharge the bootstrap capacitor, the high side MOSFET being fully ON and the low side MOSFET fully OFF.
  The charge pump is fed with a signal having a frequency of 62.5 kHz. An NPN and PNP pair is used as push-pull output stage to sink and source the necessary amount of current from and to the MOSFETs.

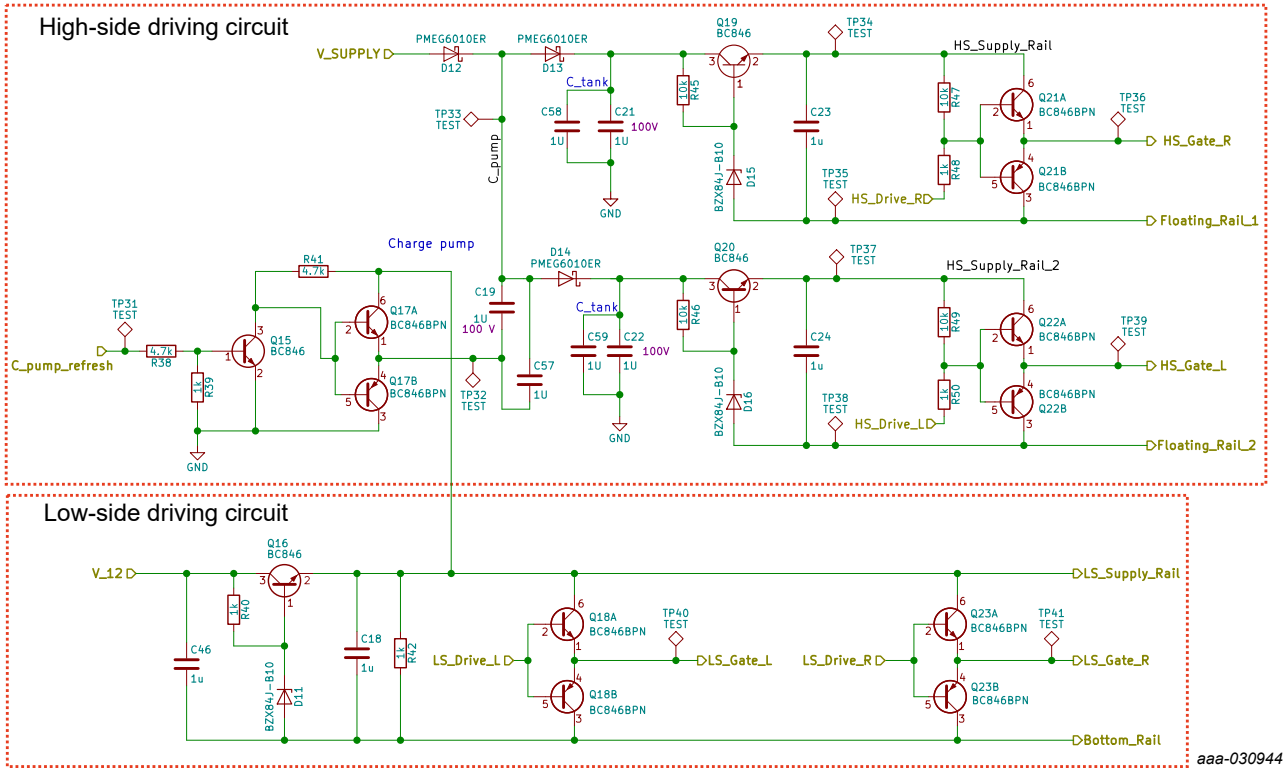

Fig. 18. H-bridge motor controller driver circuit

- **Over-current protection:** closing the control loop by means of a sensor can be really useful for monitoring and regulation purposes. In this case a resistive shunt connected in series to the return path of the H-bridge is used to limit the current flowing through the motor (to approximately 6.5 A), avoiding over dissipation in case for example of a locked rotor scenario. If the current sense voltage ends up being higher than a reference voltage the PWM function is reset and will only be reactivated if the fault disappears.
- **H-bridge:** the bridge is composed of power MOSFETs, reservoir and decoupling capacitors and snubber components. When selecting a MOSFET for this kind of application it is advisable to choose one rated for twice the expected voltage and current. Switching times can be varied by changing the gate resistance of each MOSFET, here chosen to be 10 Ω. By increasing its value the MOSFET switches slower thus further reducing any ringing, with the additional downside of increasing the switching loss of the MOSFET and the dissipation of the resistor itself. Alongside it a pull-down resistor of 10 kΩ is placed in parallel to the gate source of each MOSFET in order to completely turn off the devices when the gate voltage is low.

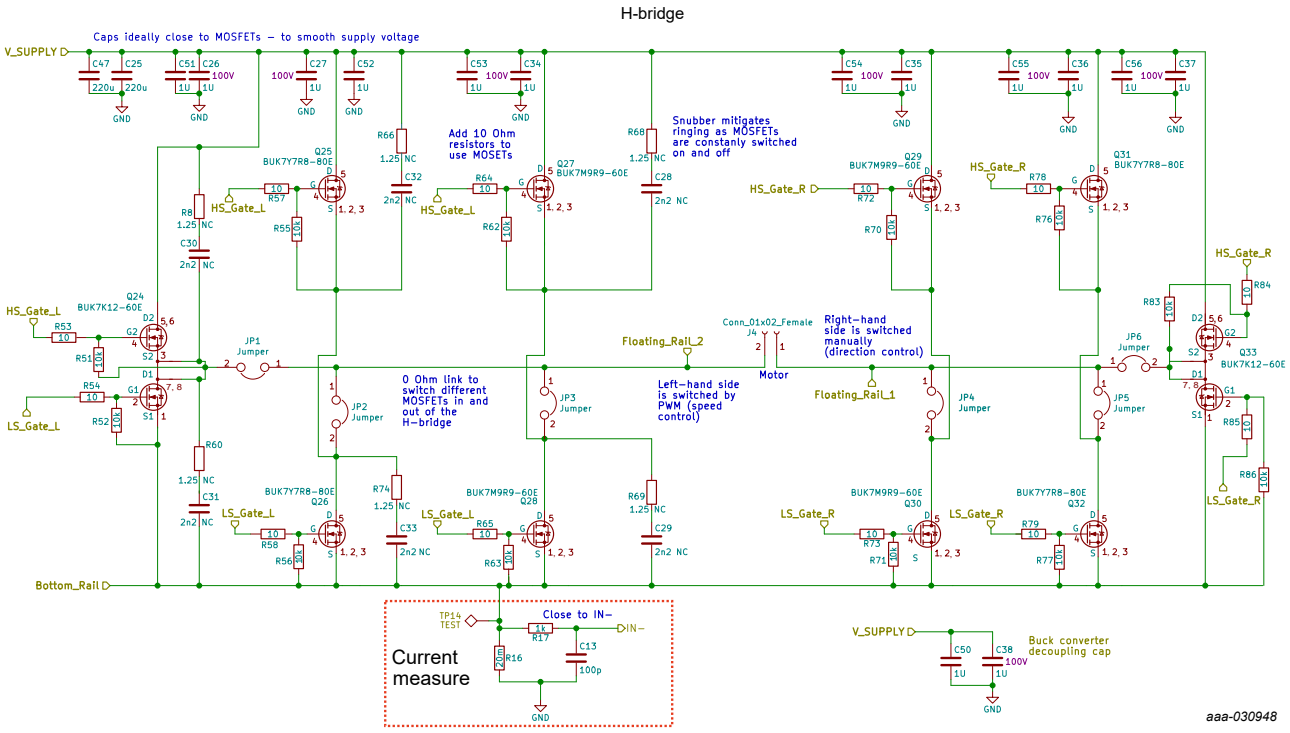

Fig. 19. H-bridge motor controller driver circuit

The design allows for different packages of power MOSFETs to be employed. The LFPAK33 provides a low-resistance in a very small-footprint packaging (3.3 x 3.3 mm), providing up to 80% space saving compared to traditional DPAK alternatives. The LFPAK56 provides a true alternative to DPAK, saving a considerable amount of space without compromising thermal performance. Packing even more into the Power-SO8 footprint the LFPAK56D fits two MOSFETs into one robust package which in case of a H-bridge offers an even smaller area and less routing parasitics. All of them are equipped with Nexperia's robust and reliable copper clip technology which allows for exceptional current handling, ultra-low package resistance and supreme robustness and reliability. Finally, many bulk capacitors are placed near the MOSFETs in order to smooth the supply voltage and absorb any voltage spike caused by the inductance of the motor. For this same reason an RC snubber may be needed in parallel to each MOSFET. Fig. 20 shows the controller driving a DC motor with a disk attached to its rotor.

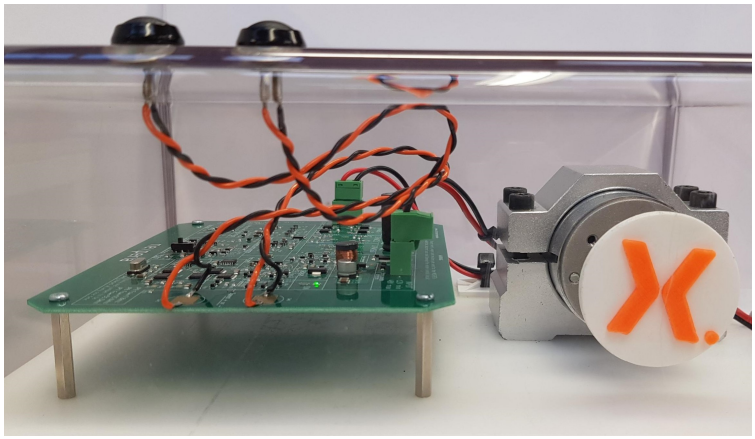

Fig. 20. Experimental setup with motor and control board

5. Circuit simulation

Based on the technical note *TN90002* and on the hardware seen in Fig. 20, the simulation in Fig. 22 was created. This focuses on the H-bridge part containing 4 Nexperia LFPAK56 MOSFETs, the BUK7Y7R8-80E. This may be seen in Fig. 21 below circled in orange.

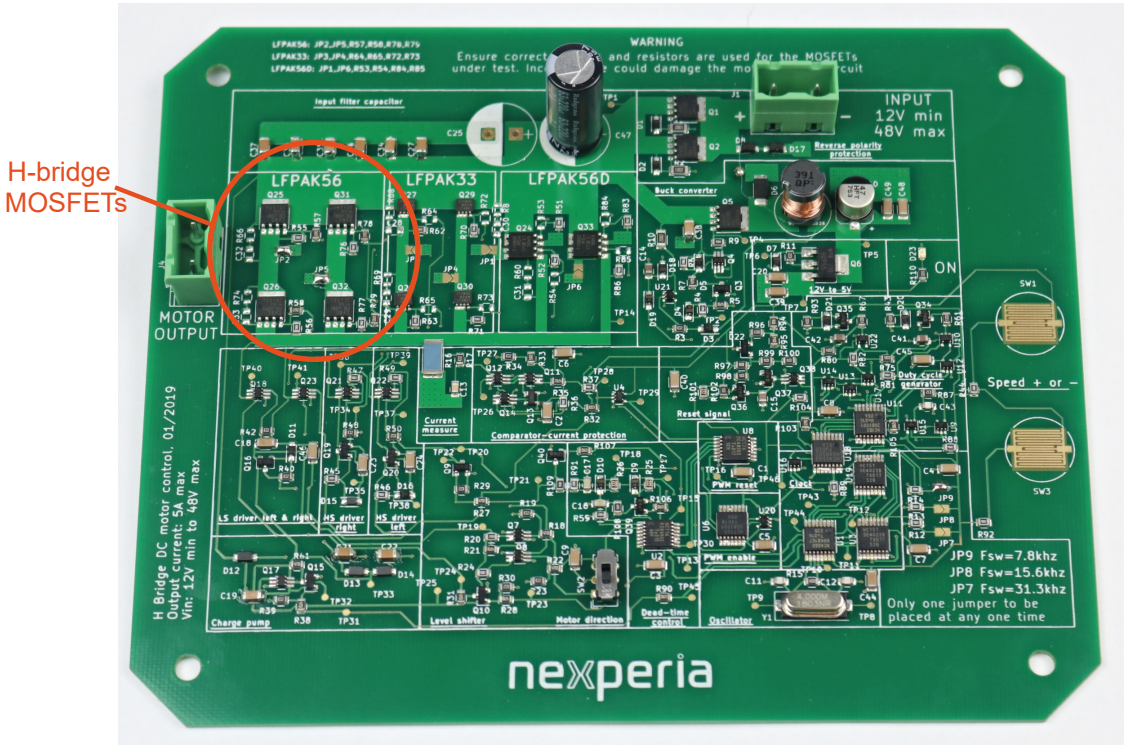

Fig. 21. Nexperia motor control PCB, H-bridge MOSFETs

The circuit schematic simulated may be seen in Fig. 22. This focused on the behaviour of the MOSFETs and thus the logic circuit was approximated using a Digital Pulse Source, a Digital Inverter, AND gates, Buffers and Digital to Voltage blocks. Additionally the PWM generators were set to one of the frequency options used in the *TN90002*, 15.6 kHz. Similarly, 10 Ω gate resistors were used.

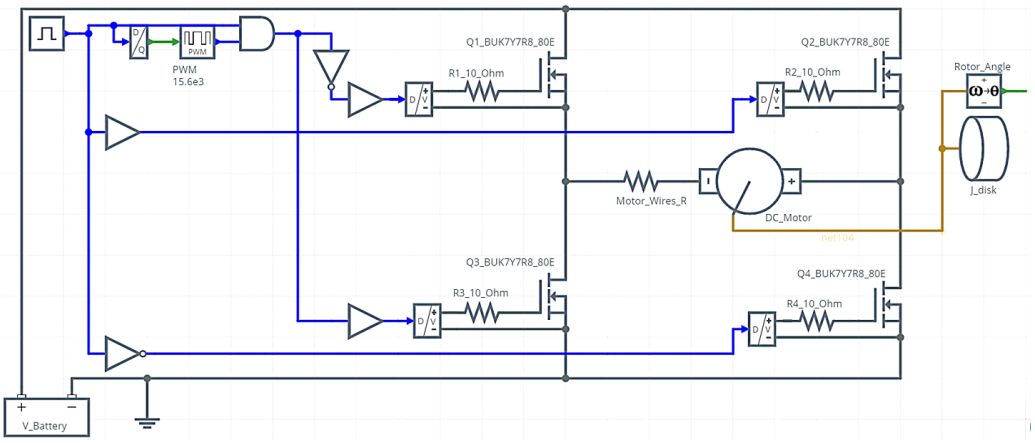

Simulation schematic

Fig. 22. Motor control, H-bridge MOSFETs simulation schematic

5.1. Logic and MOSFET gate signals

Investigating the schematic (Fig. 22) from left to right, one may see the Digital Pulse Source. This is used as an input which dictates the direction in which the motor rotates and the time for which this happens. This input signal, seen as the green trace in Fig. 23, replaces a person's interaction when using the buttons, as in *TN90002*. The logic signal is set to 1 for 150 ms. In this manner the motor is rotating clockwise. Due to this, Q2 is fully switched ON for this duration and Q3 is switched ON and OFF using the PWM generator. Moreover, Q1 was pulsed with the inverted PWM signal delivered to Q3 in order to reduce the voltage drop on the diode of Q1. In this manner the top MOSFET, Q1, is freewheeling the motor current. If this was not the case and Q1 was OFF the losses would be higher. The control signals for Q1 and Q3 may be seen in Fig. 23, as the blue and red traces whereas the ones for Q2 and Q4 may be seen as the light blue and purple traces.

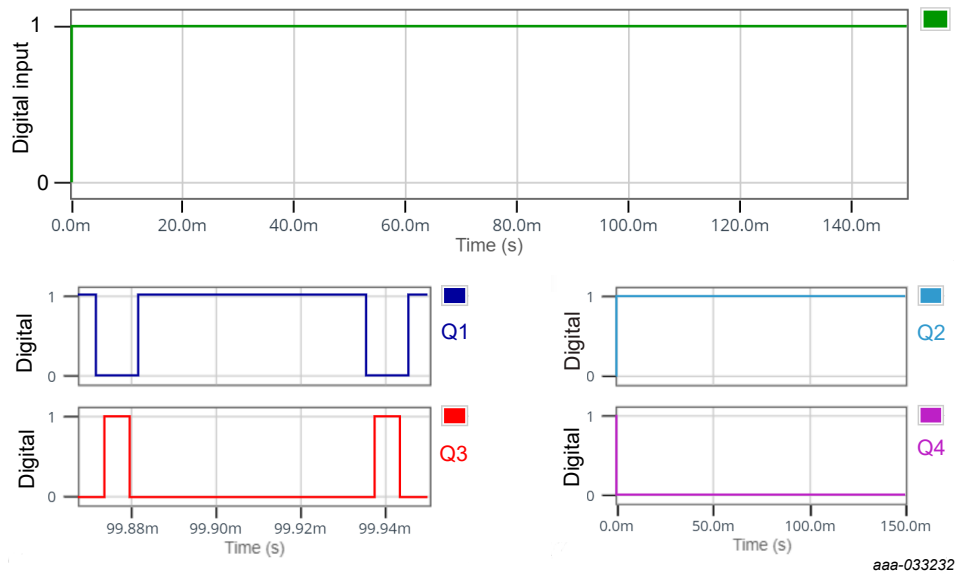

Fig. 23. Simulation waveforms; Digital Pulse Source

As mentioned in Section 3.3, dead time is mostly used when bipolar switching is implemented so that the power rails are not shorted. In this case though the unipolar scheme was used, as the left half bridge is driven by a PWM signal and its inverted version, dead time was also required. Considering the signals of Q1 and Q3 as well as for Q2 and Q4 from Fig. 23, the used dead-time was 2 µs, whereas the one set within the *TN90002* was 2.5 µs. This was implemented using the Buffer blocks seen in Fig. 22. Moreover, the 15.6 kHz PWM signal was set to a duty cycle of 12.5%.

Once the logic driving signal reached the Digital to Voltage Converter, a 10 V signal was generated in order to switch ON and OFF the four BUK7Y7R8-40E MOSFETs of the H-bridge, see Fig. 24.

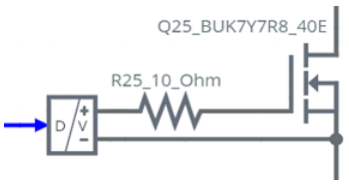

Fig. 24. Logic to voltage conversion in simulation schematic

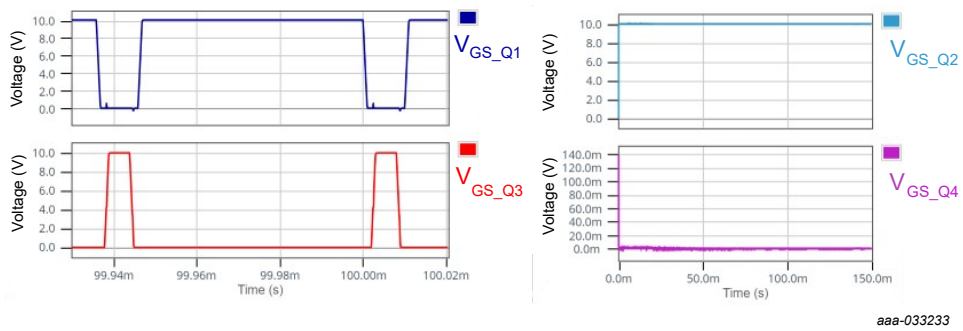

Fig. 25. Simulation waveforms: MOSFET gate voltages

In Fig. 25 the gate voltages of the respective MOSFETs of the H-bridge may be seen. The MOSFETs forming the left half-bridge, Q1 and Q3 have been switched using PWM whilst Q2 and Q4 have been switched ON or OFF fully for the respective durations. Have a closer look at the plots of V_{GS_Q1} and V_{GS_Q3}, one can again see the dead-time implementation.

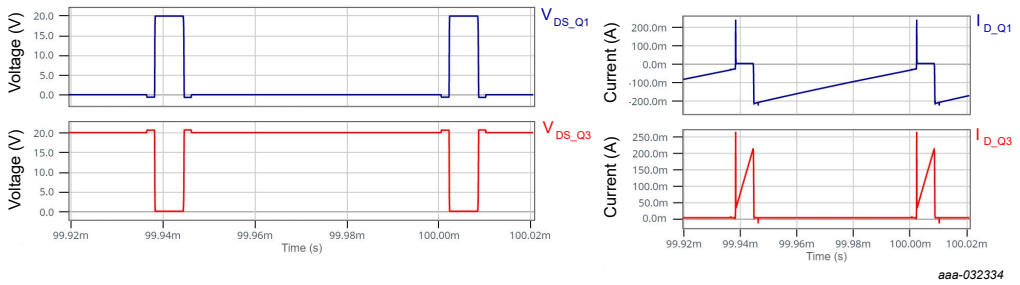

Fig. 26. Simulation waveforms: V_{DS} and I_D for Q1 and Q3

In Fig. 26 the drain source voltages of the MOSFETs within the left half-bridge may be seen as well as their respective drain currents. These have been shown for a time window of approximately 100 µs in order to focus the attention to the switching behaviour. Moreover, by multiplying the drain source voltage of Q3 by its drain current, seen in Fig. 26 the instantaneous power dissipation was obtained. Considering that this is useful to the calculation of thermal behaviour one would need to take into account the thermal time constants of the MOSFET. These time constants are bigger than the electrical time constants, for this reason, the power dissipation curve was averaged using a running average algorithm with a 1 ms window. The resulting plot may be seen in Fig. 27.

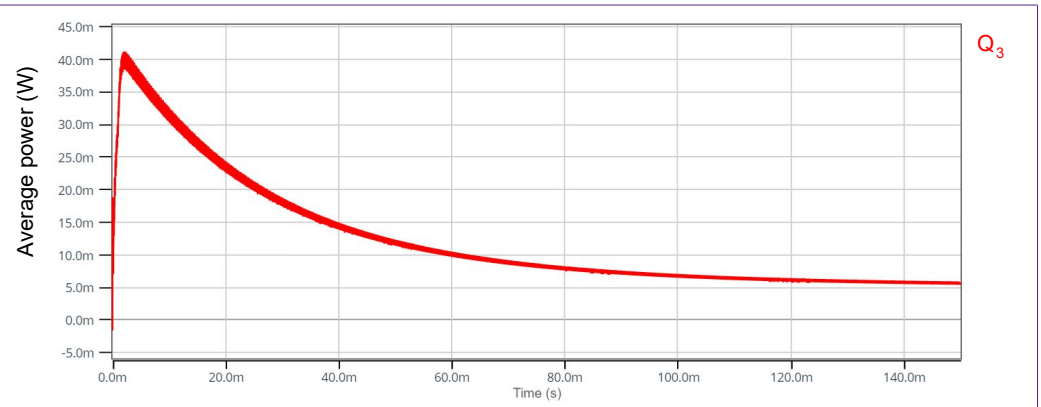

Fig. 27. Simulation waveform: average power Q3

5.2. Motor characterisation and constants

In order to simulate the behaviour of the H-bridge controller demo previously explained the motor characteristics had to be extracted so that for a specified PWM duty cycle the rotor speed in the simulation would match the one of the real application.

Considering the motor seen in Fig. 20 it was found to have the dimensions seen in Fig. 28. By measuring the rotor and by approximating its shape to a cylinder its moment of inertia was found using Eq. 20 where m = rotor mass and r = rotor radius:

$$Moment\ of\ inertia: J = \frac{1}{2} mr^2 \tag{20}$$

For this particular motor the rotor was measured to weigh 220 g and to have a radius of approximately 17 mm, thus yielding an approximately 3.15E-05 kg·m^2 moment of inertia. Additionally the plastic disc was found to have a moment of inertia of approximately 3.5E-06 kg·m^2. By adding the two the total inertia was found to be 3.5 E-05 kg·m^2.

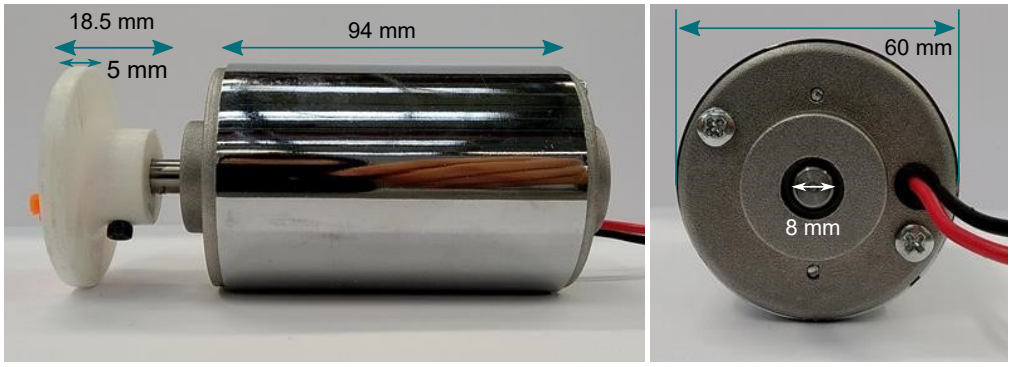

Fig. 28. DC motor dimensions

Using a DMM, the winding resistance was measured as approximately 1.5 Ω. This was also found by conducting a motor stall test and from the step response of the DC motor seen in Fig. 29.

$$Winding\ resistance: R = \frac{V_{steady\ state}}{I_{steady\ state}} = \frac{3.68\ \text{V}}{2.39\ \text{A}} \cong 1.54\ \Omega \tag{21}$$

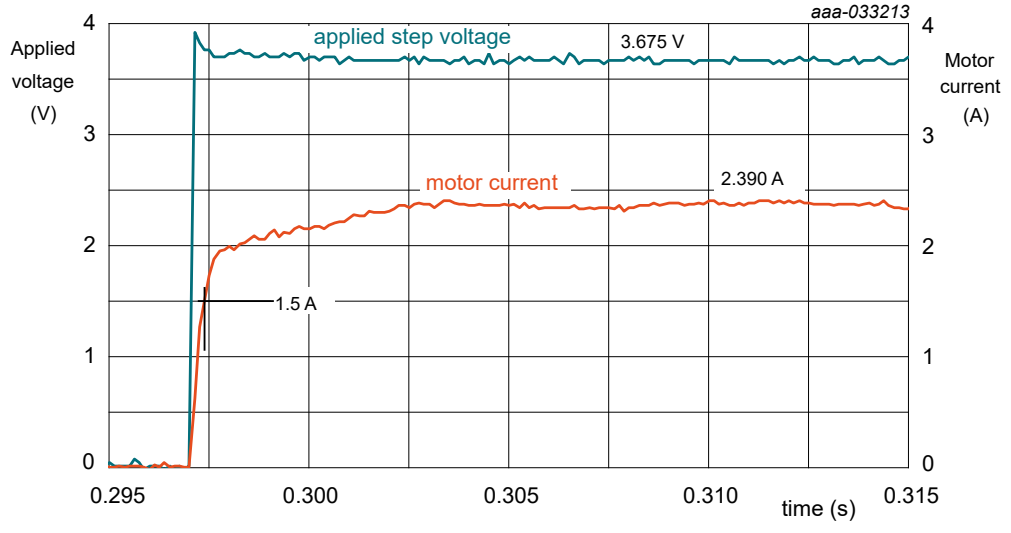

Fig. 29. DC motor step response

Additionally the electrical time constant of the motor τ, is denoted by Eq. 22, The point at which the current in Fig. 29 reaches approximately 1.5 A is when the current reaches 63.2% of its steady state value (Eq. 23, Eq. 24). This happens at approximately τ = 0.39 ms. Using the τ and the value obtained for the motor winding resistance the winding inductance was found to be approximately 600 µH.

$$Motor\ time\ constant: \tau = \frac{L}{R} \tag{22}$$

$$i(t) = I_{SS}\left(1 - e^{\frac{t}{\tau}}\right) \tag{23}$$

$$For: t = \tau \Rightarrow i(\tau) = I_{SS}\left(1 - e^{-1}\right) = 0.632\ I_{SS} \tag{24}$$

By conducting several measurements the motor's rotational speeds were found at different voltages as well as the currents and voltages. From these the motor's K_V and K_e values were inferred and thus the K_T value was found to be approximately 0.045 Nm/A.

For the DC motor the following are considered about the motor constants (Eq. 25 and Eq. 26):

$$Motor\ constants: K_T \cong K_e \tag{25}$$

$$Motor\ constants: K_V = \frac{\omega_{no\text{-}load}}{V}\ \ also:\ K_T = \frac{1}{K_V} \tag{26}$$

Lastly, another important parameter was the viscous drag which was found to be approximately 0.0001 Nm/(rad/s). At this stage the motor was characterised and thus expected to behave as the real one presented in the technical note *TN90002*.

When tested, the real system was found to achieve a rotational speed of approximately 6 RPS or 360 RPM which translated to approximately 37.7 rad/s. The board supply voltage used was 20 V, the PWM frequency, 15.6 kHz and a duty cycle of 12.5%.

Considering the circuit seen in Fig. 22 and simulating it using the mentioned motor constants, the following results were obtained:

- In Fig. 30, one may see the motor voltage and current for 3 PWM periods. These results are similar to the ones shown in Fig. 9 as well as the oscilloscope results of the real system in Fig. 31.

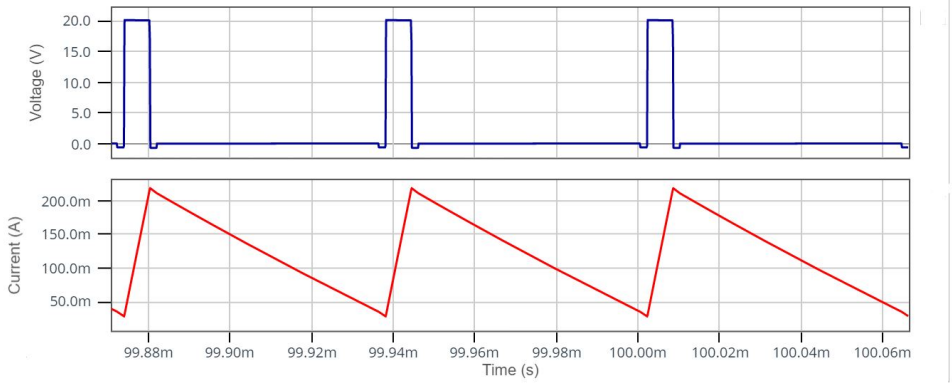

Fig. 30. DC motor voltage and current observed over 3 PWM periods

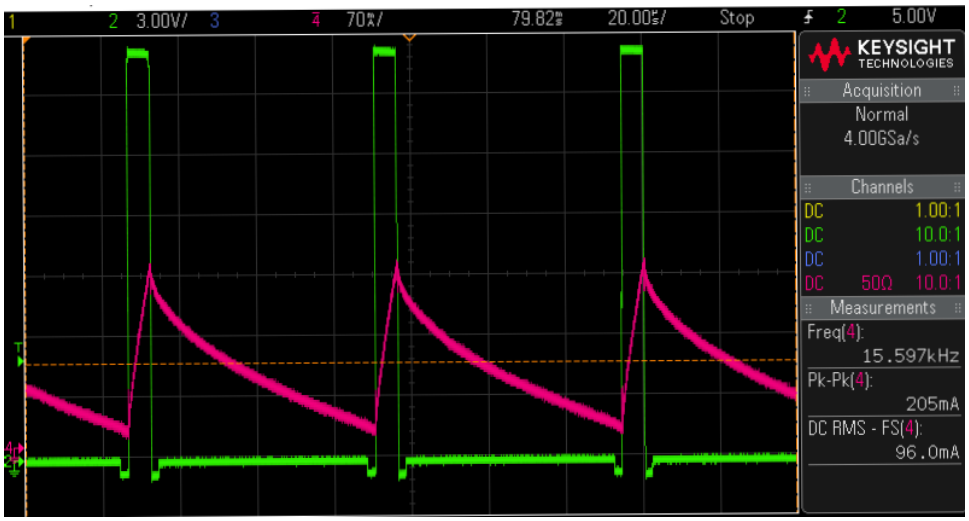

Fig. 31. Oscilloscope screen shot of motor voltage and current

- In Fig. 32, the motor steady state velocity may be seen. The rotational speed was found to be approximately 40 rad/s which is similar to the 37.7 rad/s seen in the real application from Fig. 20. Additionally the motor current and torque for the full simulation period of 150 ms may also be seen in Fig. 33.

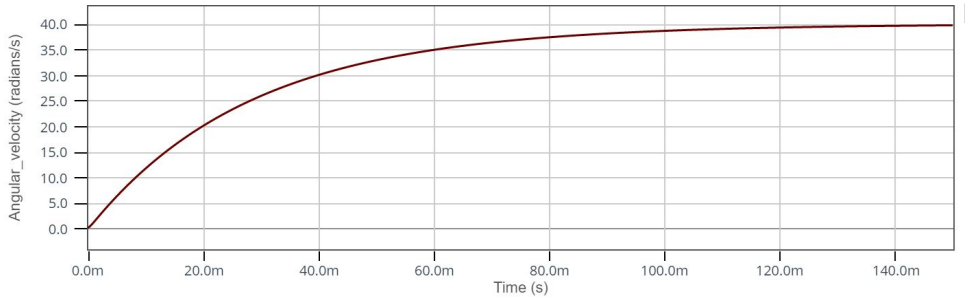

Fig. 32. DC motor simulation: angular velocity

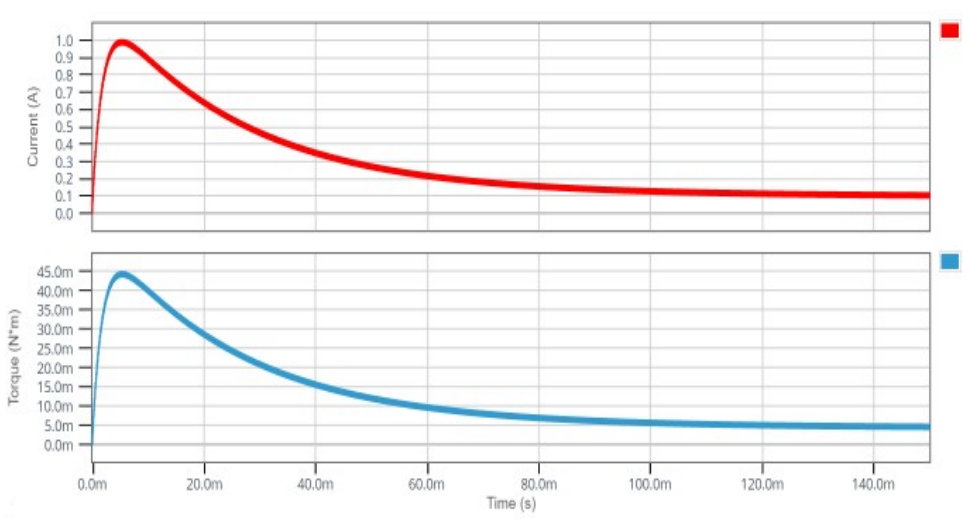

Fig. 33. DC motor simulation: current and torque

6. MOSFETs recommendations by application

Within this chapter some MOSFET recommendations will be given for applications using half-bridge and H-bridge configurations for motor control. The aimed applications are: mirror folding control, window lifter for anti-pinch function, seat control, sunroof and power tailgate control as well as fuel, water and air pumps.

6.1. Power folding mirror

In this category some MOSFETs that are recommended for this 12 V or 24 V H-bridge application are summarised in Table 4. For further explanation please refer to Section 6.1.

6.2. Window lifter for anti-pinch function

For this application the MOSFETs and system may be required to have low on-state losses, over-current protection, low thermal resistance and low thermal impedance as well as the need to be integrated into a relative small board area. The control uses PWM with frequencies ranging from 10 to 20 kHz. Motor currents of around 2 A to 5 A are expected for normal operation and operation around 10 A for shorter periods of time. In locked rotor cases, the current demand is much higher and may reach 30 A for periods ranging from 200 ms to 1 second.

6.3. Seat control

In the seat control application two motors are sometimes required, one for the forward and backwards seat adjustment and another for the backrest support adjustment. A schematic of the two H-bridges may be seen in Fig. 34. More complex circuits may be encountered in high end car models where several other motors are required in order to control things such as height, the left and right chair sides and the head rest position.

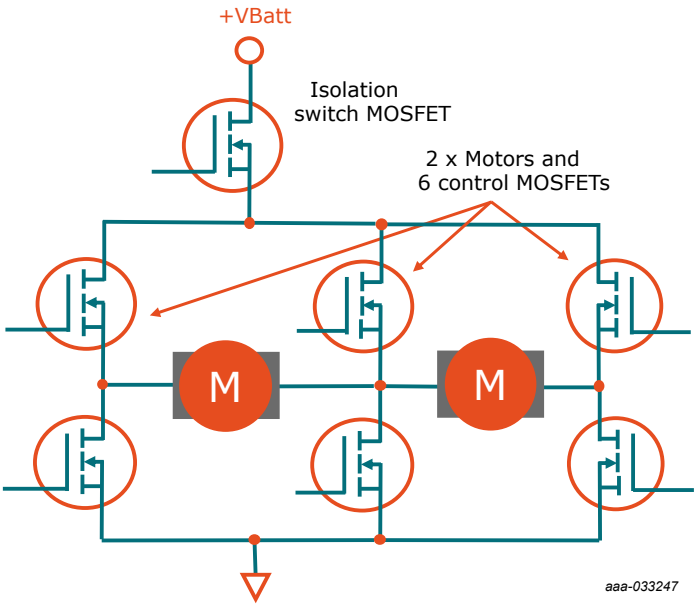

Fig. 34. MOSFETs in seat motor control application

6.4. Sunroof and power tailgate control

There are a few motors in sunroof and power tailgate applications. The motors can control the sunroof forward/backward and up/down, therefore the driving stage is required to allow bi-directionality. Both brushed and brushless DC motors can be used in this application, the former driven by a H-bridge (Fig. 35) and the latter using a multiphase half-bridge (Fig. 36). The maximum current needed for this kind of application may be around 10 A for the more power hungry ones.

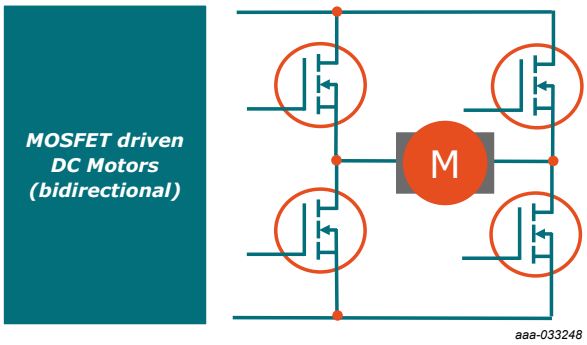

Fig. 35. H-bridge MOSFETs in sunroof motor control

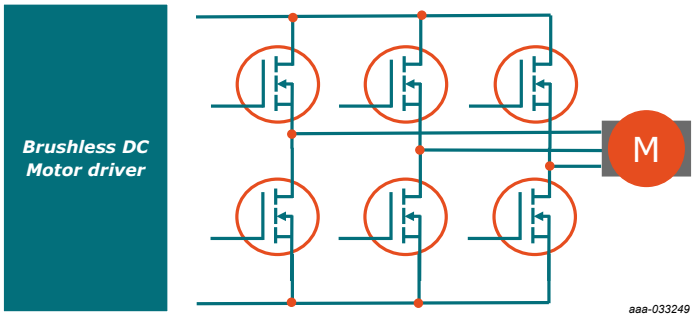

Fig. 36. 3-phase MOSFETs in sunroof motor control

6.5. Fuel, water and air pumps

There are a number of pumps used in automotive applications, such as fuel, water and air pumps. Both brushed and brushless DC motors can be suitable for this application. For the former a simple half-bridge structure can be used (Fig. 37). In some small current load applications, the recirculating FET can be replaced by a Schottky diode. For brushless motor a more complex structure of 3-phase bridge is required Fig. 36. In this case the difference in complexity and number of components can be quite stunning.

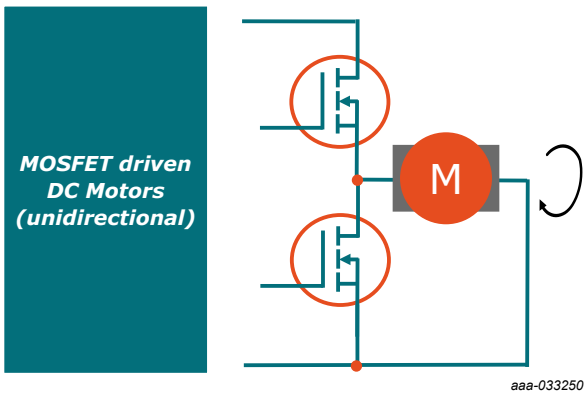

Fig. 37. MOSFETs in pump motor control applications

Since different motor applications have different power levels, from a small 30 W pump to a 300 W intake fan, the demand for power MOSFETs varies. Due to the many advantages of brushless motors more and more small water pump motors have now adopted the brushless scheme. Here, due to the large number of MOSFETs, we recommend the use of smaller packages such as the LFPAK33 and the LFPAK56D (dual devices) MOSFETs for motor drive. The 40 V device is suitable for the application of most 12 V motors. The specific model selection calls for the appropriate packaging and internal resistance, according to the load power of the motor and the overall cooling requirements of the module. Standard level V_{GS} threshold is suggested.

Table 4. Recommended MOSFETs for automotive motor control applications

Applications	System recommendations	MOSFET characteristics	MOSFET recommendations
Power folding mirror	Low on-state losses	R_{DSon}	BUK7Y3R5-40E BUK7K6R2-40E BUK9M14-60E
Window lifter for anti-pinch	Over-current protection	I_D, I_{DM}	BUK7Y4R4-40E BUK7K6R8-40E BUK7M6R0-40H
Seat control			BUK7Y3R5-40E BUK7M6R0-40H BUK7K6R2-40E
Sunroof and power tailgate control	Small footprint	LFPAK56 LFPAK56D LFPAK33	BUK7Y3R5-40E BUK7Y4R4-40E BUK7K6R2-40E BUK7M6R0-40H

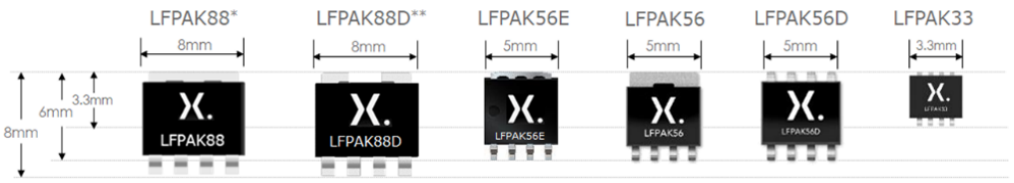

Fig. 38. LFPAK package footprint dimensions

7. Summary

The main automotive applications of DC motors have been discussed and appropriate MOSFET recommendations have been made. Nexperia offers many suitable options for most popular applications.

DC motor modelling and characterization has been presented, which can be used to better predict the performance of the driving circuitry and the selection of the necessary components. Theoretical and practical notions of H-bridge have been outlined, in particular methods of implementing PWM, motor ripple current, MOSFET dissipation and switching frequency selection.

Finally an example from the technical note *TN90002* has been presented. Its main features and operational concept have been summarized and further aspects clarified in more details.

Simulation results are included in this application note and those simulations are available for the reader to explore via the Nexperia website interactive application note pages.

8. References

1. DC Motors Speed Controls Servo Systems, Fifth Edition – Chapter 4: Speed Controls and Servo Systems – Electro-Craft Corp.
2. BUK7Y3R5-40E data sheet
3. Nexperia application note *TN90002*
4. Nexperia interactive application notes

9. Revision history

Table 5. Revision history

Revision number	Date	Description
1.1	2021-03-02	Corrections to Fig. 23 and Fig. 25.
1.0	2021-02-19	Initial version.

10. Legal information

Definitions

Draft — The document is a draft version only. The content is still under internal review and subject to formal approval, which may result in modifications or additions. Nexperia does not give any representations or warranties as to the accuracy or completeness of information included herein and shall have no liability for the consequences of use of such information.

Disclaimers

Limited warranty and liability — Information in this document is believed to be accurate and reliable. However, Nexperia does not give any representations or warranties, expressed or implied, as to the accuracy or completeness of such information and shall have no liability for the consequences of use of such information. Nexperia takes no responsibility for the content in this document if provided by an information source outside of Nexperia.

In no event shall Nexperia be liable for any indirect, incidental, punitive, special or consequential damages (including - without limitation - lost profits, lost savings, business interruption, costs related to the removal or replacement of any products or rework charges) whether or not such damages are based on tort (including negligence), warranty, breach of contract or any other legal theory.

Notwithstanding any damages that customer might incur for any reason whatsoever, Nexperia's aggregate and cumulative liability towards customer for the products described herein shall be limited in accordance with the Terms and conditions of commercial sale of Nexperia.

Right to make changes — Nexperia reserves the right to make changes to information published in this document, including without limitation specifications and product descriptions, at any time and without notice. This document supersedes and replaces all information supplied prior to the publication hereof.

Suitability for use — Nexperia products are not designed, authorized or warranted to be suitable for use in life support, life-critical or safety-critical systems or equipment, nor in applications where failure or malfunction of an Nexperia product can reasonably be expected to result in personal injury, death or severe property or environmental damage. Nexperia and its suppliers accept no liability for inclusion and/or use of Nexperia products in such equipment or applications and therefore such inclusion and/or use is at the customer's own risk.

Applications — Applications that are described herein for any of these products are for illustrative purposes only. Nexperia makes no representation or warranty that such applications will be suitable for the specified use without further testing or modification.

Customers are responsible for the design and operation of their applications and products using Nexperia products, and Nexperia accepts no liability for any assistance with applications or customer product design. It is customer's sole responsibility to determine whether the Nexperia product is suitable and fit for the customer's applications and products planned, as well as for the planned application and use of customer's third party customer(s). Customers should provide appropriate design and operating safeguards to minimize the risks associated with their applications and products.

Nexperia does not accept any liability related to any default, damage, costs or problem which is based on any weakness or default in the customer's applications or products, or the application or use by customer's third party customer(s). Customer is responsible for doing all necessary testing for the customer's applications and products using Nexperia products in order to avoid a default of the applications and the products or of the application or use by customer's third party customer(s). Nexperia does not accept any liability in this respect.

Export control — This document as well as the item(s) described herein may be subject to export control regulations. Export might require a prior authorization from competent authorities.

Translations — A non-English (translated) version of a document is for reference only. The English version shall prevail in case of any discrepancy between the translated and English versions.

Trademarks

Notice: All referenced brands, product names, service names and trademarks are the property of their respective owners.

List of Tables

List of Figures

Contents

For more information, please visit: http://www.nexperia.com
For sales office addresses, please send an email to: salesaddresses@nexperia.com
Date of release: 2 March 2021